Korean J. Chem. Eng., 33(8), 2298-2307 (2016)
DOI: 10.1007/s11814-016-0111-9

pISSN: 0256-1115
eISSN: 1975-7220

Large-scale calculation of hydrodynamic transport properties for random suspensions of hard-sphere particles

Sangkyun Koo†

Department of Chemical Engineering and Materials Science, Sangmyung University, Seoul 03016, Korea
(*Received 28 December 2015 • accepted 22 April 2016*)

Abstract−A numerical method based on fast multipole summation scheme is used to calculate hydrodynamic interactions in random suspensions of non-colloidal hard-sphere particles. The calculation is carried out for suspensions of 1,024 particles randomly placed in periodic unit cell to determine hydrodynamic transport properties such as permeability of a viscous flow through porous medium, effective viscosity of suspension, and sedimentation velocity of the suspended particles. The particle volume fraction ϕ ranges from 0.01 to 0.25. Effect of particle number N on the transport properties was examined through the numerical calculations with N=64-1,024. It is shown that sedimentation velocity increases with N approaching an estimate for infinite N, and the finite N effect is negligible in effective viscosity and permeability problems. The present scheme is quite useful for obtaining a statistically-averaged quantity for random suspensions. As an example, ensemble-averaged velocity when position of one particle is fixed is numerically obtained in sedimentation problem. The numerical results are shown to be in excellent agreement with theoretical prediction.

Keywords: Hard-sphere Suspension, Fast Summation Algorithm, Conditional Ensemble Average, Multipole Expansion, Stokes Flow

INTRODUCTION

Particulate suspensions are found in many industrial applications as slurries, pastes, colloids, and composites. It is important to understand macroscopic transport properties and behavior of the suspensions in handling the suspensions for various applications. The macroscopic transport properties typically include permeability of fluid flowing through porous medium, effective viscosity of suspension, hydrodynamic diffusion coefficient, and sedimentation velocity of suspended particles. The macroscopic properties and behavior are influenced by various forces such as Brownian, electrostatic, dispersion, hydrodynamic, and other external forces acting on the suspended particles. When the suspensions are subjected to flow, the hydrodynamic force acting on the particles plays a predominant role in determining the transport properties and behavior of the suspension. The hydrodynamic force is caused by imposed flow and its perturbation due to the presence of the suspended particles. Since the contribution of the imposed flow to the hydrodynamic force is straightforward, the contribution of the flow perturbation is considered more significant. Flow perturbation is determined from a complicated calculation of the hydrodynamic interactions among the particles. The calculation employs a spatially periodic lattice structure to simulate the suspensions. The lattice points are assumed to extend periodically. This periodic unit volume with a lattice point is called a unit cell. The lattice point is considered as the center of suspended particles for ordered arrays such as simple cubic, body-centered cubic, and face-centered cubic arrays. Numerical simulation of the hydrodynamic interactions for suspension systems starts from single particle in unit cell, i.e., ordered arrays of the particles. To see various phenomena and average properties of random suspensions, it is needed to include multiple particles in unit cell. Many studies have been performed to solve the problems of multiple particles in a unit cell [1-9]. Multiparticle problems require more complex and expensive calculations. Hence, much effort has been devoted to devising an efficient calculation scheme.

Significant progress was made by Durlofsky et al. [3] and Brady and Bossis [4]. They presented an efficient calculation scheme which splits hydrodynamic interaction into near-field and far-field interaction depending on distance from the particle at origin. Computationally, this scheme is an $O(N^3)$ algorithm for N particles in unit cell. Later, some methods for fast calculation were reported. These fast calculation methods enabled us to handle a large number of particles. Ladd [10,11] has shown an O(N) approach based on statistical mechanics. He developed a lattice-Boltzmann technique in which continuous fluid phase is replaced by lattice-Boltzmann gas particles. His calculation was for random suspensions of only 16 particles to determine hydrodynamic transport properties, although other analysis in his paper was performed up to 1,024 particles. Traditional analysis based on continuum mechanics was also made by Sangani and Mo [12], who suggested an O(N) scheme using a fast multipole summation method based on Greengard's algorithm [13,14]. However, they provided relatively few results, and some of the results seem to have poor convergence. More recently, Sierou and Brady [15] incorporated a particle-mesh-Ewald algorithm [16] to the $O(N^3)$ calculation scheme developed by Brady and Bossis [4]. Conventional Ewald summation technique was modified with the particle-mesh approach to calculate far-field interaction in an efficient manner, reducing the calculation cost to $O(N\ln N)$. This algo-

†To whom correspondence should be addressed.
E-mail: skkoo@smu.ac.kr

rithm, however, is inherently slower than the previously developed O(N) schemes [10,12].

In present study, numerical calculation of hydrodynamic interaction in random suspensions is carried out on a large scale with N=1,024 non-colloidal particles in unit cell. The calculation is based on a multipole expansion method in which flow perturbation due to presence of particles is expressed in terms of multipoles. For this large scale calculation, a fast multipole expansion method by Sangani and Mo [12] is used, which combines a fast summation technique with multipole expansion method. Poor convergence in their calculations [12] is improved in the present study by examining convergence behavior. This large-scale calculation is used to determine not only hydrodynamic transport properties but also statistically averaged quantities of random suspensions. Typical examples of the hydrodynamic transport properties are the permeability of a viscous fluid flowing through porous medium, effective viscosity of suspension, and sedimentation velocity of suspended particles. These properties are calculated in the present study for dilute and semi-dilute random suspensions with particle volume fraction ϕ ranging from 0.01 to 0.25. The large-scale calculation enables us to determine the effect of particle number N on the transport properties. The particle number effect is examined with numerical simulation for N=64-1,024 in the present study.

The advantage of the present large-scale calculation is to obtain statistically averaged quantities of random suspensions. Ensemble average when one particle is fixed, i.e., conditional ensemble average, is well used to conceptually analyze flow behavior in random suspensions. Mean-field theories such as effective-medium theories have been developed to determine the macroscopic properties and behavior of random suspensions by approximation of conditional averages using simple models which capture important physics for fluid behavior. Actually, numerical calculation of the conditional averages has been seldom done. The large-scale scheme in the present study makes it possible to calculate a conditional average. Numerical calculation of conditionally ensemble-averaged velocity is performed in sedimentation problems. The numerical results are compared with theoretical prediction from an effective-medium theory.

FORMULATION AND NUMERICAL METHOD

1. Formulation

Consider a suspension of spherical particles in a viscous fluid. The motion of the particles is governed by various forces acting on the particles. The forces can also directly influence fluid flow and the fluid flow exerts hydrodynamic force on the particles in turn. When particle Peclet number for the flow is large, hydrodynamic force acting on the particles becomes dominant. The hydrodynamic force results from imposed flow and its perturbation due to the presence of particles. At a particle Reynolds number of the fluid flow much less than unity, the fluid flow satisfies the Stokes equation. To simulate infinite particle systems, it is assumed that N particles are placed in periodic unit cell as shown in Fig. 1. The general solutions to the Stokes equation for the periodic unit cell system are expressed by the Green function G_{ij} and its successive derivatives. Using the Einstein notation, the general solutions are given by

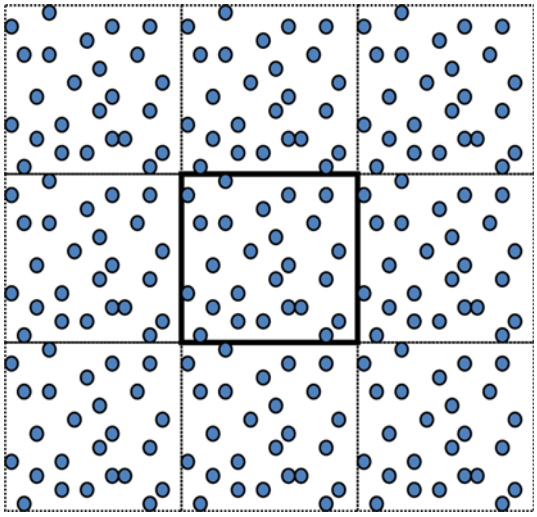

Fig. 1. Schematic diagram for periodic unit cell. Filled circles are particles and thick-lined square in the center indicates the unit cell considered in present study.

$$u_i(\mathbf{x}) - u_i^{\infty}(\mathbf{x}) = \sum_{\alpha=1}^{N} (A_j^{\alpha} + B_{jk}^{\alpha}\partial_k + C_{jkl}^{\alpha}\partial_{kl}^2 + \cdots) G_{ij}(\mathbf{x} - \mathbf{x}^{\alpha}), \tag{1}$$

where u_i is the fluid velocity and u_i^{∞} is the superficial velocity by imposed flow. The notation $\mathbf{x}$ is the position vector and $\mathbf{x}^{\alpha}$ denotes the position of particle α. The coefficients A_j^{α}, B_{jk}^{α} and C_{jkl}^{α} are the multipoles. The Green function G_{ij} is written in terms of spatially periodic fundamental solutions S_1 and S_2

$$G_{ij}(\mathbf{x}) = \frac{-1}{4\pi\mu}\left(S_1(\mathbf{x})\delta_{ij} - \frac{\partial^2 S_2(\mathbf{x})}{\partial x_i \partial x_j}\right), \tag{2}$$

where

$$S_m(\mathbf{x}) = \frac{(-4\pi^2)}{\pi\tau}\sum_{\mathbf{k}\neq\mathbf{0}} k^{-2m}\exp(-2\pi i\mathbf{k}\cdot\mathbf{x}), \quad m=1, 2. \tag{3}$$

Here, τ is the volume of unit cell and $\mathbf{k}$ is the reciprocal lattice vector. The multipoles are directly related to the force F_i, the torque L_i, and the stresslet S_{ij} acting on a sphere α. The fluid velocity in Eq. (1) also satisfies Lamb's general solution for Stokes flow around spheres [18]. Lamb's general solution around a sphere α is given by

$$\mathbf{u}(\mathbf{r}) = \sum_{n=1}^{\infty}[c_n r^2 \nabla p_n^{\alpha} + b_n \mathbf{r} p_n^{\alpha} + \nabla\times(\mathbf{r}\chi_n^{\alpha}) + \nabla\Phi_n^{\alpha}], \tag{4}$$

where $c_n = \dfrac{-n+2}{2n(2n-3)}$ and $b_n = \dfrac{n+1}{n(2n-3)}$.

Here, $r=|\mathbf{r}|=|\mathbf{x}-\mathbf{x}^{\alpha}|$ is the distance from the center of the sphere α and p_n^{α}, c_n^{α} and Φ_n^{α} are the n^{th}-order spherical harmonics consisting of singular and regular harmonics. The harmonic p_n^{α}, is written as the sum of its singular and regular harmonics, which are distinguished by superscripts s and r, respectively. The singular harmonics is given by

$$p_n^{s,\alpha} = \sum_{j=0}^{1}\sum_{m=0}^{n} P_{nm}^{j,\alpha} Y_{nm}^{j} r^{-2n-1}, \tag{5}$$

$$Y_{nm}^{0} = r^n P_n^m(\cos\theta)\cos m\varphi, \; Y_{nm}^{1} = r^n P_n^m(\cos\theta)\sin m\varphi. \tag{6}$$

The regular harmonics is

$$P_n^{r,\alpha}=\sum_{j=0}^{1}\sum_{m=0}^{n} P_{nm}^{rj,\alpha}Y_{nm}^{j}, \tag{7}$$

with c_n and b_n replaced by c_{-n-1} and b_{-n-1}. The notations $P_{nm}^{j,\alpha}$ and $P_{nm}^{rj,\alpha}$ denote the coefficients of singular and regular harmonics, each. The function $P_n^m(\cos\theta)$ is the associated Legendre polynomial function. The spherical azimuthal and polar angles θ and φ are taken with respect to x_1 axis as polar axis. For the harmonics χ_n^α, $T_{nm}^{j,\alpha}$ and $T_{nm}^{rj,\alpha}$ are the singular and regular coefficients. Likewise, $\Psi_{nm}^{j,\alpha}$ and $\Psi_{nm}^{rj,\alpha}$ are the singular and regular coefficients for Φ_n^α. These regular coefficients are all written in terms of the singular coefficients and the derivatives of S_1 and S_2 in Eq. (3) [7]. For example, $P_{nm}^{rj,\alpha}$ is given by

$$P_{nm}^{rj,\alpha}=(-2)^m[(1+\delta_{m0})(n+m)!]^{-1}\sum_{\beta=1}^{N}[\mathscr{D}_{nm}^{j}(\mathbf{x}\cdot\mathscr{G}^{\beta}\nabla^2-\nabla\cdot\mathscr{G}^{\beta})]S_1(\mathbf{x}^\alpha-\mathbf{x}^\beta), \tag{8}$$

where $\mathscr{D}_{nm}^{j}$ and $\mathscr{G}^{\beta}$ are the differential operators given by the Eqs. (A1)-(A3) and Eqs. (A7)-(A9), respectively, in the Appendix. We use differentiation properties of $\mathscr{D}_{nm}^{j}$ obtained by Hobson [19]. Some examples are presented in Eqs. (A4)-(A6). Detailed expressions for $T_{nm}^{rj,\alpha}$ and $\Psi_{nm}^{rj,\alpha}$ are given in Mo and Sangani [7].

Lamb's coefficients, which are matched to the multipoles in Eq. (1), also directly give the expressions for the forces and the stresslets on each sphere [7,17]:

$$\begin{aligned}&F_1^\alpha=-4\pi\mu P_{10}^{0,\alpha},\ F_2^\alpha=4\pi\mu P_{11}^{0,\alpha},\ F_3^\alpha=4\pi\mu P_{11}^{1,\alpha},\\ &S_{11}^\alpha=-4\pi\mu P_{20}^{0,\alpha}/3,\ S_{12}^\alpha=2\pi\mu P_{21}^{0,\alpha},\ S_{13}^\alpha=2\pi\mu P_{21}^{1,\alpha},\\ &S_{22}^\alpha=4\pi\mu(P_{20}^{0,\alpha}/6-P_{22}^{0,\alpha}),\ S_{23}^\alpha=-4\pi\mu P_{21}^{0,\alpha},\ S_{33}^\alpha=2\pi\mu(P_{20}^{0,\alpha}/6+P_{22}^{0,\alpha}).\end{aligned} \tag{9}$$

Therefore, numerical calculation is carried out to determine the singular coefficients by applying boundary conditions for each sphere. It is convenient to use u_r, $\nabla_s\cdot\mathbf{u}_s$, $\mathbf{e}_r\cdot(\nabla\times\mathbf{u}_s)$ in spherical coordinate for the boundary conditions. Here, u_r and $\mathbf{u}_s$ $(=u_\theta\mathbf{e}_\theta+u_\varphi\mathbf{e}_\varphi)$ are the radial and the tangential velocity at the surface of sphere, respectively. The operator ∇_s is defined by $\nabla_s=r(\nabla-\mathbf{e}_r\partial/\partial r)$. Rearranging these boundary conditions in terms of the singular and regular coefficients of harmonic functions in Eq. (4), we obtain

$$\Psi_{nm}^{rj,\alpha}+\frac{(n+1)a^{-2n+1}}{n(2n-1)(2n+1)}P_{nm}^{j,\alpha}+\frac{a^2}{2(2n+1)}P_{nm}^{rj,\alpha}=P_{nm}^{j,\infty} \tag{10}$$

$$\Psi_{nm}^{j,\alpha}-\frac{a^2}{2(2n+1)}P_{nm}^{j,\alpha}+\frac{na^{2n+3}}{(n+1)(2n+1)(2n+3)}P_{nm}^{rj,\alpha}=\Psi_{nm}^{j,\infty}, \tag{11}$$

$$T_{nm}^{rj,\alpha}+T_{nm}^{j,\alpha}a^{-2n-1}=T_{nm}^{j,\infty}, \tag{12}$$

for the superscript j=0 and 1. The right-hand sides of the above equations are obtained from the imposed boundary conditions given in terms of u_r, $\nabla_s\cdot\mathbf{u}_s$, $\mathbf{e}_r\cdot(\nabla\times\mathbf{u}_s)$. The regular coefficients on the left-hand side include the singular contribution from all the other particles than the particle α.

The above equations finally give an overall matrix **Ax=b** where the matrix **A** contains configuration-dependent coefficients for a set of linear equations with the singular coefficients taken as independent variables, i.e., solution vector **x**. The vector **b** is given from imposed boundary conditions. A parallel programming is implemented for accelerating calculation.

2. Numerical Method

Overall numerical calculation consists of two steps. The first is to calculate the periodic Green functions S_1 and S_2 and their derivatives as functions of distance between the particle at origin and all the other particles, which finally enables us to determine contribution of singular coefficients for all the surrounding particles to regular coefficients for the particle at origin. Ewald summation method is used for evaluating the S_1 and S_2 in the infinite space [21]. The singular contributions to regular coefficients together with the boundary conditions are used to form a set of linear equations in which the singular coefficients are the unknowns. Then, the second step is to solve the set of linear equations using an iterative method. We use a generalized minimum residual method, which reduces the computation cost of $O(N^3)$ to $O(N^2)$ as an iterative matrix solver.

Computation of the Green functions as functions of interparticle distance is the most costly in the overall calculation. Hydrodynamic interaction between particles is directly related to determining the regular coefficients, which include singular contributions from all the particles except a particle at origin. The singular contributions are given in terms of a sum of the Green functions for all the interparticle distance between the particle at origin and all the other particles. Since this summation is carried out over all pairs of the particles, the computation becomes considerably costly. Hence, it is necessary to perform this pair-wise summation more efficiently to reduce the overall calculation cost. An efficient way is grouping of singular contributions from particles in a distant region, i.e., far-field interaction. The grouping is carried out so that the singular coefficients for particles in a distant region are translated to those for the center of the region. We use Green's identity and Laplacian of harmonic functions for translation of singular coefficients. Using mathematical properties of spherical harmonics and their derivatives, we obtain the formulas for translating singularities from low to high level [12,19,20]. For example, $P_{nm}^{j,L}$ at lower level is translated to $P_{nm}^{j,H}$ at higher level using the following Eq. (13)

$$P_{nm}^{j,H}=\varepsilon_{nm}\lambda_{nm}\sum_{i=0}^{1}\sum_{k=1}^{\infty}\sum_{l=0}^{k}\lambda_{kl}^{-1}P_{kl}^{i,L}\mathscr{D}_{kl}^{i}Y_{nm}^{j}(\mathbf{x}^H-\mathbf{x}^L), \tag{13}$$

where $\varepsilon_{nm}=\dfrac{(-2)^m}{(1+\delta_{m0})(n+m)!}$, $\lambda_{nm}=(-1)^{n-m}(n-m)!2^{1-m}$.

Through the translation and summation, singular coefficients for particles in a region can be represented simply by those for the center of the region. The grouping is performed in a hierarchical manner, from small (low level) to large (high level) region. Hence, it requires virtual, multi-level partition of unit cell space. This virtual partition is done in proportion to number of particles, creating many small sub-cells. The proper number of partitions should be chosen so that the smallest sub-cells contain the particles of approximately O(1). As the hierarchical level becomes high, the sub-cell size becomes larger and then we have fewer sub-cells in a unit cell. The minimum number of the sub-cells is practically 64. This hierarchical grouping is needed for far-field interaction. For near-field interaction, the hydrodynamic interaction is calculated in pair-

wise and particle-to-particle manner. The near-field interaction is applied to closest neighbors in 27 (=3×3×3) sub-cells at equal level. Thus a hierarchical grouping is used beyond this distance. At the highest hierarchical level of 64 sub-cells, the singular coefficients for the sub-cells in far field contribute to the regular coefficients for the sub-cells where the particle at the origin is located. The regular coefficients for all the sub-cells of the highest level are determined. Then the next is to determine the regular coefficients at the lower level, which are given by the sum of singular contribution at the equal level and regular contribution translated from the higher level which replace far-field interaction beyond closely neighboring sub-cells at the equal level. Translation of regular coefficients from high level to low level is quite similar to that of the singular coefficients. For example, $P_{nm}^{rj,H}$ at higher level is translated to $P_{nm}^{rj,L}$ at lower level with Eq. (14)

$$P_{kl}^{ri,L}=\varepsilon_{kl}\sum_{j=0}^{1}\sum_{n=1}^{\infty}\sum_{m=0}^{k}P_{nm}^{ri,H}\mathscr{O}_{kl}^{i}Y_{nm}^{j}(\mathbf{x}^{L}-\mathbf{x}^{H}). \quad (14)$$

Therefore, at the lowest level, i.e., at the largest number of sub-cells, the regular coefficients are determined from singular contributions from closely located particles or sub-cells and translated regular contributions from the higher level. This hierarchical grouping and translation scheme finally enables us to determine the regular coefficients of sub-cells at all levels, including the individual particles, which reduces computation cost of pairwise calculation for all pairs of particles.

This calculation scheme also makes it possible to calculate statistical quantities such as conditional ensemble average, which is used to describe the average properties for random configurations. Ensemble average with one particle fixed is termed as conditional ensemble average. The conditional ensemble average is a theoretical basis for developing mean-field theory such as effective-medium theory. Effective-medium theories were developed to estimate hydrodynamic transport properties using simple models. Due to the fast calculation scheme, the fluid velocity can be numerically obtained as a function of distance from test particle, which corresponds to conditionally ensemble-averaged velocity. The detailed calculation results are given in the following Section.

An IBM machine, GAIA in supercomputing center of Korea Institute of Science and Technology Information, was used for numerical computations. Most computations implemented with MPI (message passing interface) for parallel computing were conducted with 16 processors of the IBM machine. Computing time was less than 10 seconds for the hydrodynamic property of one configuration of 1,024 particles at ϕ=0.1.

RESULTS AND DISCUSSION

1. Convergence and Tolerance Check

To solve matrix **Ax=b**, an infinite set of Eqs. (10)-(12) needs to be truncated to a finite number of equations. The truncation should be optimized to both satisfy low computation cost and high accuracy. An efficient truncation scheme [7] is used for n≤Ns for Eq. (10), n≤Ns-2 for Eq. (11) and n≤Ns-1 for Eq. (12). The total number of the equations, $(3Ns^2-1)N$, is determined by choosing Ns. Truncation is also necessary in translating the singular and regular coefficients for hierarchical grouping. For the translation a new parameter Nt is used instead of Ns. The parameter Nt is chosen similarly to Ns and Nt≥Ns. With properly chosen Ns and Nt, the average drag acting on particles was calculated for a random array including 1,024 particles at particle volume fractions ϕ of 0.15 and 0.25, respectively. The results are shown in Fig. 2(a) and 2(b). Since hydrodynamic interaction between particles becomes stronger with particle concentration, larger Ns is needed for higher concentrations of particles. The cases of Ns=2 for both concentrations seem to lack accuracy compared with those of Ns=3 and 4. Most calculation results in a previous study by Sangani and Mo [12] were presented for the case of Ns=2. At Ns=2; fluctuation is observed for Nt=2 and 3. This fluctuation is rapidly reduced with increasing Ns. For both concentrations the condition of Ns=3 and Nt=5 is acceptable. Hence the numerical calculations in the present study were performed at Ns=3 and Nt=5 or higher Ns. At the test runs for Ns and Nt, error tolerance for matrix calculation was chosen as 0.0001. The error tolerance ε is defined as the square root of Euclidean norm of (**b**−**Ax**) normalized by **b**, i.e. $\varepsilon=\sqrt{\|\mathbf{b}-\mathbf{A}\cdot\mathbf{x}\|/|\mathbf{b}|}$. Fig. 3 shows calculation results for drag force acting on particles in a random array with ε ranging from 0.01 to 0.00001. It is seen that

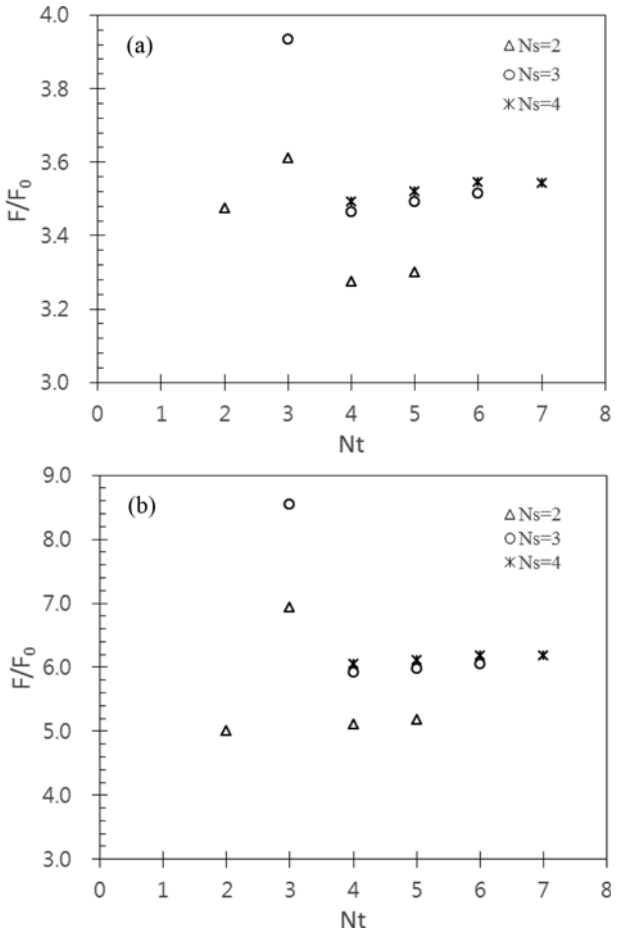

Fig. 2. Normalized drag force F/F_0 at various Ns and Nt with ε= 0.0001. The average drag force F is taken for 20 configurations of 1,024 particles and F_0 denotes the drag for an isolated particle. (a) ϕ=0.15 and (b) ϕ=0.25.

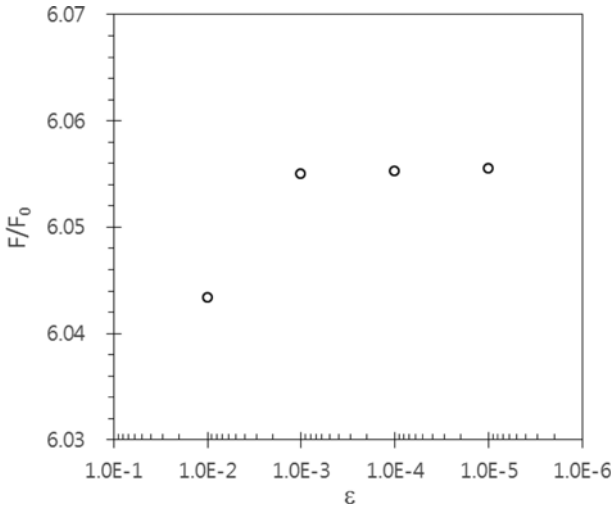

Fig. 3. Normalized drag force (F/F_0) at various ε with Ns=3 and Nt=6.

the drag force values saturate at ε=0.001 and the smaller ε. Hence the error tolerance ε is set to be 0.001 or 0.0001 in most calculations. This check is also valid in viscosity and sedimentation problems [22].

2. Large N Calculation for Hydrodynamic Transport Properties

With the properly chosen parameters of Ns, Nt and ε, numerical calculations were performed for 20 individual random arrays of 1,024 particles at various ϕ to determine sedimentation velocity, effective viscosity, and drag force for suspensions in random arrays. Commonly, the particle volume fraction ϕ ranges from 0.01 to 0.25, and no-slip boundary condition is applied on the surface of particles for the problems. The computations were successfully performed and the results were all compared with previous results by Ladd [6] for N=16 and 108 and Sangani's group [7,12] for N=16 and 1,024. Comparison with Sierou and Brady [15] is also presented to show the effect of N on sedimentation velocity as well as agreement of both results.

The sedimentation problem is considered first. Particles settle through a viscous fluid due to density difference between particle and fluid under gravity. In sedimentation and viscosity problems, additional 6N equations are included for force and torque balance. For the settling particles, gravitational force is balanced by hydrodynamic force, which is directly related to multipoles and hence the corresponding singular coefficients. The calculation results for N=1,024 are given and compared with those from previous work in Fig. 4. The sedimentation velocity U normalized by Stokes' velocity for an isolated particle U_0 is plotted as a function of ϕ. It is seen that the normalized sedimentation velocity data are spread at each ϕ. In particular, Sangani and Mo's result [12] for N=1,024 gives much lower value of the sedimentation velocity. This is attributed to lack of accuracy due to low Ns and Nt in their calculation. More importantly, the sedimentation velocity increases with N. In sedimentation problems it has been known that the sedimentation velocity has N dependency due to difference in the limiting behavior of random and ordered array at low ϕ and lack of hydrodynamic screening. Hence, corrections have been made to yield theoretical estimate for infinite N [6,7]. Mo and Sangani [7] obtained an expression for infinite N correction of the sedimentation velocity

$$U(\infty) = U(N) + \frac{1.7601}{\mu^*/\mu}\left(\frac{\phi}{N}\right)^{1/3} S(\mathbf{0})U_0 + O\left(\frac{\phi}{N}\right), \quad (15)$$

where μ^* and μ are the viscosity of suspension and fluid at given ϕ. The notation $S(\mathbf{0})$ is the structure factor at zero-wavenumber limit and can be estimated by Carnahan-Sterling approximation for hard-

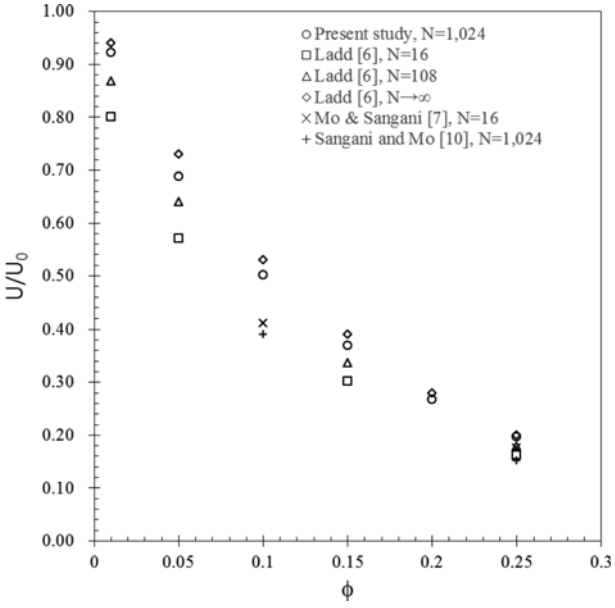

Fig. 4. Normalized sedimentation velocity U/U_0 at ϕ=0.01-0.25. The average sedimentation velocity U is taken for 20 random configurations of 1,024 particles and U_0 is the sedimentation velocity for an isolated particle.

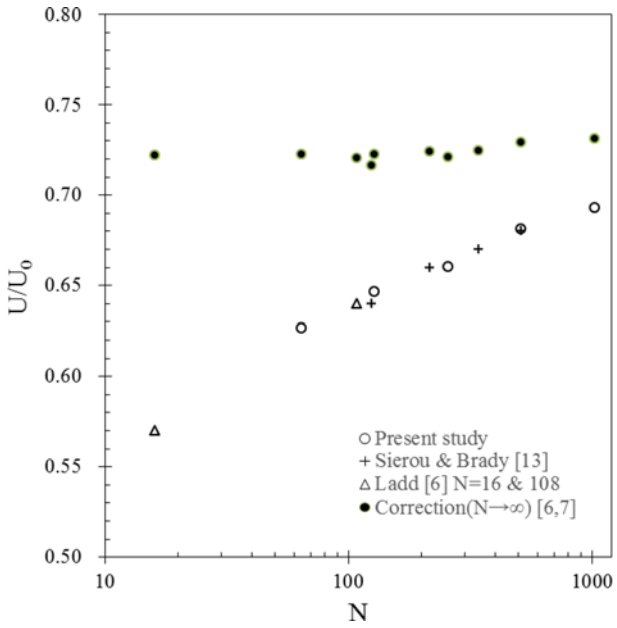

Fig. 5. Normalized sedimentation velocity U/U_0 as a function of the number of particles N.

sphere systems:

$$S(\mathbf{0}) = \frac{(1-\phi)^4}{1+4\phi+4\phi^2-4\phi^3+\phi^4}. \quad (16)$$

Sedimentation velocity for infinite N has been calculated from that for various N ranging from 16 to 1,024 at ϕ=0.05 using Eq. (15). In addition to the sedimentation velocity data from simulation, the previous data by Sierou and Brady [15] and Ladd [6] are also included for comparison. Fig. 5 shows that the estimates for infinite N from these simulation data for each N fall on 0.72-0.73 at ϕ=0.05. It is confirmed that the sedimentation velocity follows N dependency in Eq. (15). It is also observed that the simulation results agree well with those by Sierou and Brady [15].

As an important advantage, large N calculation can be used to calculate statistical averages such as conditional ensemble average and radial distribution function. The conditional ensemble average, i.e., ensemble average subject to the presence of a particle at origin, provides essential basis for expressing average quantities for the random arrays. The equations of motion and fluid properties such as density and viscosity can be written in terms of conditional ensemble average. For example, the density is given by

$$\rho(\mathbf{x}) = \rho_f + (\rho_p - \rho_f)\langle\zeta\rangle_1(\mathbf{x}|\mathbf{0}). \quad (17)$$

where $\rho(\mathbf{x})$ is the density at $\mathbf{x}$, ρ_f and ρ_p are the density of fluid and particle, respectively, and ζ is a phase indicator function whose value is unity when $\mathbf{x}$ lies inside a particle and zero otherwise. The notation $\langle\zeta\rangle_1(\mathbf{x}|\mathbf{0})$ is the conditional ensemble average of ζ defined by

$$\langle\zeta\rangle_1(\mathbf{x}|\mathbf{0}) = \int_{|\mathbf{x}-\mathbf{x}'|\le a} P(\mathbf{x}'|\mathbf{0})\,dV_{\mathbf{x}'} \quad (18)$$

where $P(\mathbf{x}'|\mathbf{0})$ is the probability density for finding a particle with its center at $\mathbf{x}'$ given the presence of a particle at the origin $\mathbf{0}$. Note that ζ approaches ϕ as $|\mathbf{x}|\to\infty$. The conditional averages of pressure and velocity are required to approach their unconditional ensemble averages as $|\mathbf{x}|\to\infty$.

The present numerical scheme for large N can be used to numerically obtain the conditional ensemble averages. This scheme is based on hierarchical structure in a unit cell containing N particles. The unit is virtually subdivided into many sub-cells. For N=1,024, number of the smallest sub-cells is 512. Since velocity of fluid or particle at each center of the smallest sub-cells is calculated from this numerical calculation, the velocity can be obtained as a function of the distance from the center of the smallest cell to each particle in the whole unit cell, as schematically shown in Fig. 6. For one random array of 1,024 particles, 512×1,024 data points are obtained.

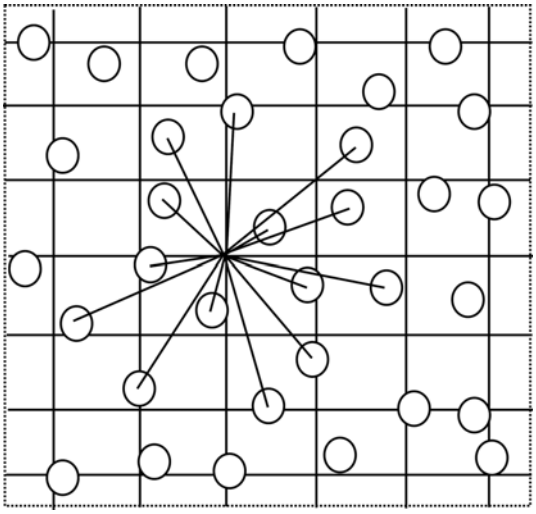

Fig. 6. Numerical scheme for conditional ensemble-average. Fluid velocity at each grid point is plotted as a function of distances between the grid point and centers of all particles. This plotting is repeated for all grid points. Using this scheme the averaged fluid velocity is statistically obtained as a function of distance from the test particle at origin.

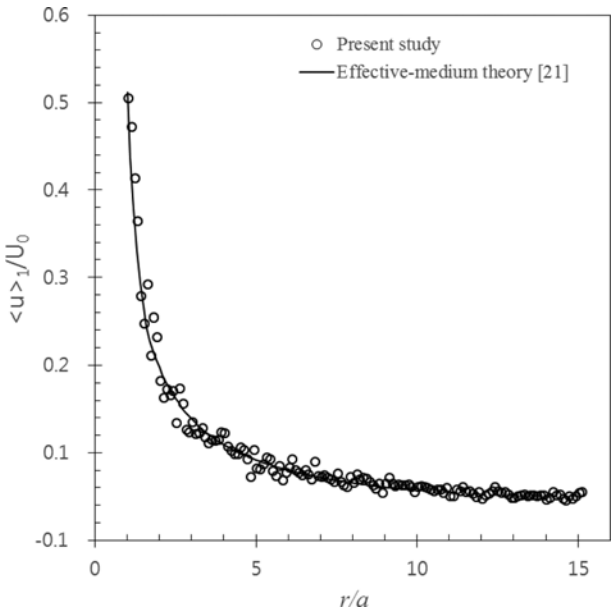

Fig. 7. Conditional ensemble average of sedimentation velocity $\langle u\rangle_1$ normalized by U_0 as function of non-dimensional distance r/a from the test particle at origin.

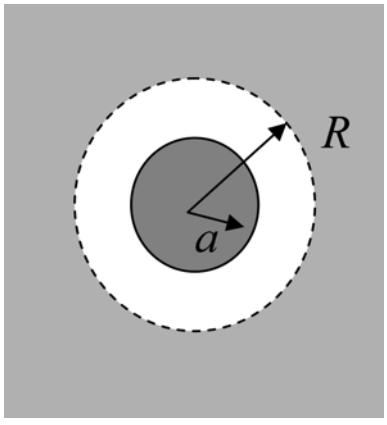

Fig. 8. Schematic diagram for an effective-medium model [21]. A test particle is surrounded by clear fluid up to the distance R beyond which an effective medium exists.

Averaging these data over 20 random arrays yields the conditional ensemble average of velocity as a function of the distance from a test particle at origin. Fig. 7 shows the conditionally averaged velocity $<u_1>_1(\mathbf{x}|\mathbf{0})$ of a settling test particle with the distance from center of the particle for 20 random arrays at ϕ=0.1. This numerically obtained conditional average is compared with theoretical prediction from effective-medium theory based on the concept of conditional ensemble average. The effective-medium theory usually portrays suspensions as consisting of test particle at origin and surrounding effective-medium, which is a self-consistent mean filed approximation. We employ an effective-medium theory developed by Dodd et al. [23] to estimate sedimentation velocity. This model is shown in Fig. 8, where the test particle at origin is surrounded by clear fluid up to distance R beyond which an effective medium exists. The test particle represents individual particles. Near field around the test particle is up to the distance R and the effective medium is considered as far field. Velocity and stress in the both fields should be continuous at R for self-consistency. Consideration of volume exclusion effect near the test particle gives the distance R

$$R = a\left(\frac{1-S(\mathbf{0})}{\phi}\right)^{1/3}, \tag{19}$$

The settling velocity of the test particle is determined from continuities of velocity and stresses at r=a and r=R together with force balance between gravity and viscous drag. These estimations are plotted as a solid line in Fig. 7 for comparison with the above numerical results. The theoretical estimations agree very well with the numerical results.

Next, we deal with viscosity and permeability problems. The viscosity problem is to calculate stresslets on each particle and hence to determine the effective viscosity of suspensions under simple shear or extensional flow. The effective viscosity for isotropic hard-sphere suspensions is given by

$$\mu^* = \mu(1+nS), \tag{20}$$

where μ^* and μ are the viscosity of suspension and fluid and n is the number density of particles. Average stresslet $<S_{ij}>$ is equal to $2Se_{ij}$ with e_{ij} being rate of strain tensor. Additional equations for force and torque balance on particles are considered as in sedimentation problem. The stresslets are also directly obtained from singular multipole coefficients $P_{nm}^{j,\alpha}$ as given in Eq. (9). The results are presented in Fig. 9. The calculation results are in good agreement with previous work at low ϕ below 0.15. Fig. 10 shows the effect of N on the suspension viscosity at ϕ=0.05. The calculation results are compared with Ladd's result for N=16-108. It is confirmed that the number of particles does not affect suspension viscosity. At ϕ=0.25, however, the present study shows lower value of viscosity than the previous work does. It is attributed to lack of lubrication calculation in the present study. For lubrication flow, i.e., fluid flow in the gap between particles in close proximity, fluid velocity and force density change steeply in the gap. Accurate calculation for this case requires exceptionally high number of Ns, which enormously increases overall computation cost. Hence, incorporation of efficient calculation for lubrication is necessary for large N calculation for problems where the lubrication calculation is important. The lubrication effect is usually negligible at low ϕ, but it becomes significant at moderate to high ϕ, particularly in viscosity problems.

Lastly, we calculate the average drag force acting on stationary particles for a given mean flow and hence determine Darcy's permeability k_p defined by

$$\mu\langle\mathbf{u}\rangle = -k_p\nabla\langle p\rangle \tag{21}$$

Since $-\nabla\langle p\rangle = n\langle\mathbf{F}\rangle$ with n being the number density of particles and

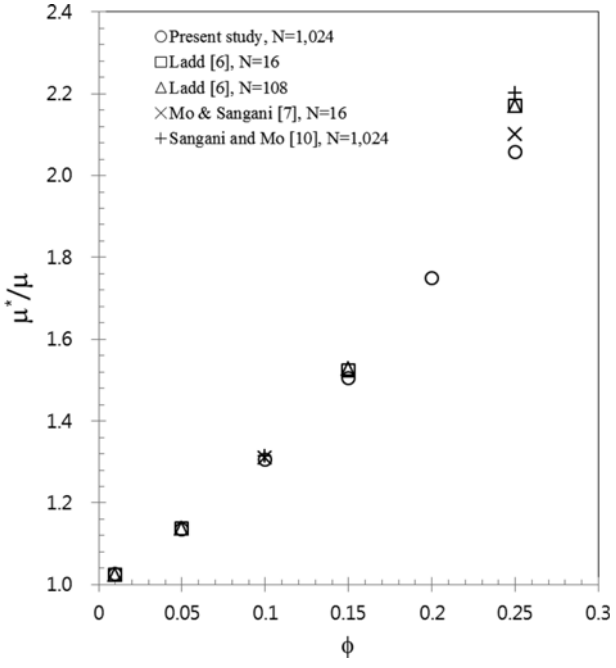

Fig. 9. Normalized effective viscosity μ^*/μ at ϕ=0.01-0.25. The effective viscosity of suspension μ^* is taken for 20 random configurations of 1,024 particles and μ is the fluid viscosity.

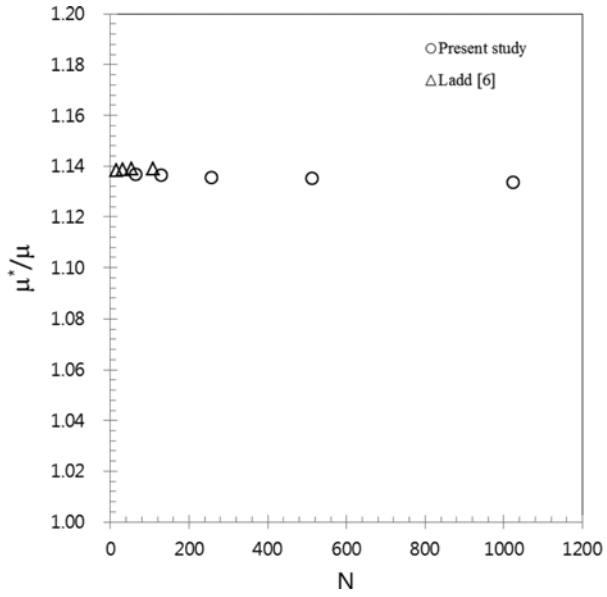

Fig. 10. Normalized effective viscosity μ^*/μ as a function of the number of particles N.

$$\langle \mathbf{F} \rangle = 6\pi\mu a \langle \mathbf{u} \rangle K = \langle \mathbf{F}_0 \rangle K, \quad (22)$$

$$k_p = \frac{2a^2}{9\phi K}. \quad (23)$$

Here, K is the non-dimensional drag which accounts for multi-particle effect, and $\langle \mathbf{F}_0 \rangle$ is the drag force acting on an isolated particle. Since the particles are fixed, the additional equations for force and torque balance are not included in this problem. The drag force results from mean flow and its perturbation due to the presence of particles. Evaluation of the flow perturbation requires calculation of the hydrodynamic interaction and determining singular multipole coefficients. The drag force is the average of force dipoles on particles as in Eq. (9). The calculation results for K are given in Fig. 11. It is shown that K for N=16 and 108 from Ladd [6] is slightly larger than the present calculation result for N=1,024. Finite N effect is checked with numerical calculation for N=64 to 1,024 at ϕ=0.05. Fig. 12 shows that K at N=64 is larger than that for N=1,024 by 2.4%, which is considered as negligible N effect. However in this figure it seems that in Ladd's results K for N=16 exhibits larger difference from that for N=108. It was shown that this difference reduced rapidly as ϕ increased and there was negligible effect of finite N.

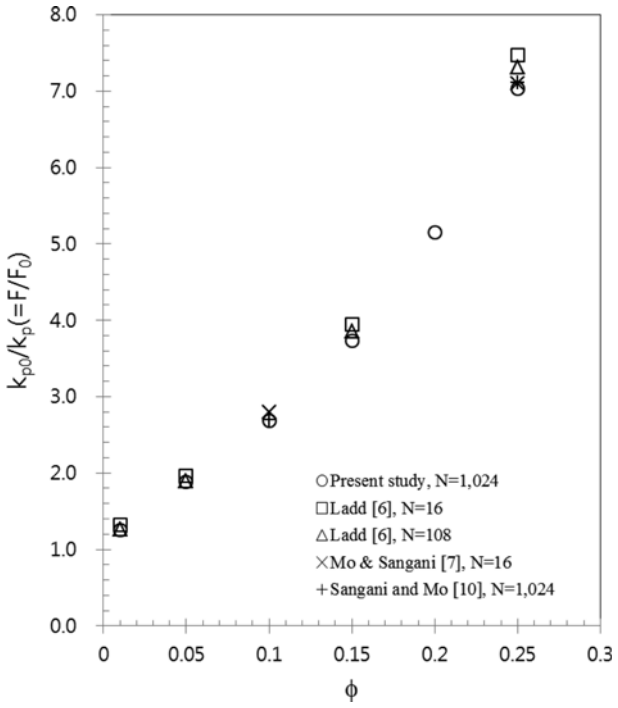

Fig. 11. Normalized Darcy's permeability k_{p0}/k_p (=F/F_0) at ϕ=0.01-0.25. The average permeability k_p is taken for 20 random configurations of 1,024 particles and k_{p0} is the permeability for an isolated particle.

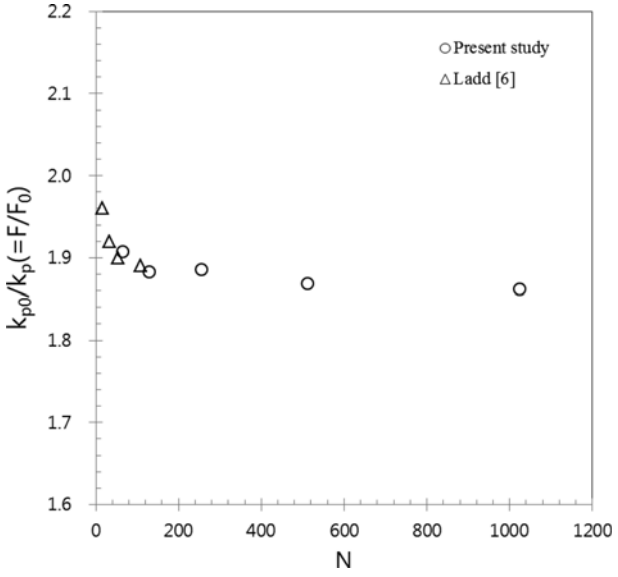

Fig. 12. Normalized Darcy's permeability k_{p0}/k_p (=F/F_0) as a function of the number of particles N.

CONCLUSION

A fast multipole summation scheme was used to calculate hydrodynamic interactions in random suspensions containing N=1,024 hard-sphere particles in unit cell, and hence to determine hydrodynamic transport properties such as Darcy's permeability in porous medium, effective viscosity of suspension, and sedimentation velocity of suspended particles. The numerical calculation was performed for ϕ=0.01-0.25. The transport properties of random suspensions were obtained by taking averages over 20 particulate configurations at each ϕ.

Finite N effect on the hydrodynamic transport properties was investigated through a numerical calculation with N=64-1,024. It is shown that the sedimentation velocity for finite N increases with N, and its corrections for infinite N agree very well with theoretical estimations. These results are consistent with previous results by Sierou and Brady [15]. The effect of N was negligible in viscosity and permeability problems.

The present calculation method was also used to numerically obtain conditional ensemble-average for random configurations of suspensions, which is the ensemble average when one particle is fixed. The conditionally averaged velocity in sedimentation problem was presented as a function of distance from a particle at the origin. This numerical result was compared with estimations from an effective-medium theory developed by Dodd et al. [23]. Both results were in excellent agreement. It has been shown that the fast calculation scheme is quite useful to numerically obtain statistical average of random suspensions.

ACKNOWLEDGEMENT

This work was supported by National Research Foundation of Korea Grant funded by the Korean Government (Grant No. 2011-0010934). Computations were performed using the supercomputer facilities provided by Korea Institute of Science and Technology Information (KSC-2013-C1-015).

NOMENCLATURE

a : radius of particle

$\mathbf{e}_r$, $\mathbf{e}_\theta$, $\mathbf{e}_\varphi$: unit vectors in the radial, azimuthal and polar angle direction, respectively
$\mathbf{F}$, F_i : force acting on particle
F_0 : force acting on an isolated particle
$\mathbf{k}$: reciprocal lattice vector
k_p : Darcy's permeability
G_{ij} : Oseen tensor (Green's function)
L_i : torque acting on particle
N : number of particles in periodic unit cell
Ns : truncation order for a set of Eqs. (14)-(16)
Nt : truncation order for translating singular and regular coefficients
n : number density of particles
$P(\mathbf{x}|\mathbf{0})$: probability of finding a particle at $\mathbf{x}$ given a particle at origin $\mathbf{0}$
p : pressure
$\mathbf{r}$, r : radial position vector, radial distance from the center of the particle at origin, $r=|\mathbf{r}|$
R : exclusion distance from the origin to the effective-medium boundary
$S(\mathbf{0})$: structure factor at zero wavenumber limit for hard-sphere suspension
S_1, S_2 : spatially periodic fundamental solution, $\nabla^2 S_1 = S_2$
S_{ij} : stresslet acting on particle
U : sedimentation velocity of particles in a fluid
U_0 : sedimentation velocity of an isolated particle in a fluid
$\mathbf{u}$, u_i : velocity of the fluid
$\mathbf{x}$: position vector
Y_{nm} : surface harmonics function

Greek Letters

δ : delta function (Kronecker delta function)
μ, μ^* : viscosity of fluid and suspension
ϕ : volume fraction of particles in unit cell
$\rho(\mathbf{x})$: density at position $\mathbf{x}$ in suspension
ρ_f, ρ_p : density of fluid and particle
τ : volume of unit cell
ζ : phase indicator function of particle
$\langle\zeta\rangle_1$: pair probability density, conditional ensemble average of ζ

REFERENCES

1. P. Mazer and W. van Saaloos, *Physica A*, **115**, 21 (1982).
2. C. W. J. Beenakker, *Physica A*, **128**, 48 (1984).
3. G. Bossis and J. F. Brady, *J. Chem. Phys.*, **80**, 5141 (1984).
4. L. Durlofsky, J. F. Brady and G. Bossis, *J. Fluid Mech.*, **180**, 21 (1987).
5. J. F. Brady and G. Bossis, *Annu. Rev. Fluid Mech.*, **20**, 111 (1988).
6. A. J. C. Ladd, *J. Chem. Phys.*, **93**, 3484 (1990).
7. G. Mo and A. S. Sangani, *Phys. Fluids*, **6**, 1637 (1994).
8. A. A. Zaidi, T. Tsuji and T. Tanaka, *Korean J. Chem. Eng.*, **32**, 617 (2015).
9. C. Wang, Z. Zong and X. Wang, *Korean J. Chem. Eng.*, **32**, 2384 (2015).
10. A. J. C. Ladd, *J. Fluid Mech.*, **271**, 285 (1994).
11. A. J. C. Ladd, *J. Fluid Mech.*, **271**, 311 (1994).
12. A. S. Sangani and G. Mo, *Phys. Fluids*, **8**, 1990 (1996).
13. L. Greengard and V. Rokhlin, *J. Compu. Phys.*, **73**, 325 (1987).
14. L. Greengard, *Science*, **265**, 909 (1994).
15. A. Sierou and J. F. Brady, *J. Fluid Mech.*, **448**, 115 (2001).
16. R. W. Eastwood and J. W. Hockney, *Computer simulation using particles*, I.O.P. Publishing, Philadelphia (1988).
17. S. Kim and S. J. Karrila, *Microhydrodynamics*, Butterworth-Heinemann, Boston (1991).
18. H. Lamb, *Hydrodynamics*, Dover, New York (1945).
19. E. W. Hobson, *The theory of spherical and ellipsoidal harmonics*, Cambridge University Press, Cambridge (1931).
20. A. S. Sangani and A. Acrivos, *Int. J. Multiphase Flow*, **8**, 343 (1982).
21. H. Hasimoto, *J. Fluid Mech.*, **5**, 317 (1959).
22. S. Koo, *Korean J. Chem. Eng.*, **28**, 364 (2011).
23. T. L. Dodd, D. A. Hammer, A. S. Sangani and D. L. Koch, *J. Fluid Mech.*, **293**, 147 (1995).

APPENDIX

The differential operator $\mathscr{D}^j_{nm}$ is defined by

$$\mathscr{D}^j_{nm} = \Delta^j_m \frac{\partial^{n-m}}{\partial x_1^{n-m}}, \quad (j=0,\ 1), \tag{A1}$$

$$\Delta^0_m = \left[\left(\frac{\partial}{\partial\xi}\right)^m + \left(\frac{\partial}{\partial\eta}\right)^m\right], \quad \Delta^1_m = i\left[\left(\frac{\partial}{\partial\xi}\right)^m - \left(\frac{\partial}{\partial\eta}\right)^m\right], \tag{A2}$$

$$\xi = x_2 + ix_3, \quad \eta = x_2 - ix_3. \tag{A3}$$

We can use properties of $\mathscr{D}^j_{nm}$, which was obtained by Hobson [17]. The relevant formulas have been summarized by Acrivos and Sangni [18] and Sangani and Mo [10]. Some examples are as follows:

$$\mathscr{D}^j_{nm} r^{-1} = \lambda_{nm} r^{-2n-1} Y^j_{nm}, \quad \lambda_{nm} = (-1)^{n-m}(n-m)!\,2^{1-m} \tag{A4}$$

$$\mathscr{D}^j_{kl} Y^j_{nm} = \begin{cases} c_1 Y^0_{n-k,\,m+l} + c_2 Y^0_{n-k,\,|m-l|}, & \text{for } i+j\neq 1 \\ c_1 Y^1_{n-k,\,m+l} + c_2 \dfrac{m-l}{|m-l|}(-1)^i Y^1_{n-k,\,|m-l|}, & \text{for } i+j=1 \\ \varepsilon^{-1}_{nm}, & \text{for } i=j,\ n=k,\ m=l \end{cases} \tag{A5}$$

$$c_1 = (-1)^{ij} 2^{-l} \frac{(n+m)!}{(n-k+m+l)!}, \quad c_2 = (-1)^{\min(m,\,l)} \frac{2^{-l}(n+m)!}{(n-k+|m-l|)!}, \quad \varepsilon_{nm} = \frac{(-2)^m}{(1+\delta_{m0})(n+m)!}. \tag{A6}$$

The differential operator $\mathscr{G}^\beta$ is expressed in terms of singular coefficients [7]:

$$\mathscr{G}^\beta_1 = \sum_{n=1}^{\infty}\sum_{m=0}^{n} \frac{1}{\lambda_{nm}} \left\{ m\left(-T^{1,\alpha}_{nm}\mathscr{D}^0_{nm} + T^{0,\alpha}_{nm}\mathscr{D}^1_{nm}\right) - \frac{(n-m)(n+m)}{n(2n-1)}\left(P^{0,\alpha}_{nm}\mathscr{D}^0_{nm} + P^{0,\alpha}_{nm}\mathscr{D}^1_{nm}\right) \right\} \tag{A7}$$

$$\mathscr{G}^\beta_2 = \sum_{n=1}^{\infty}\sum_{m=0}^{n} \frac{1}{\lambda_{nm}} \left\{ (n-m)(1+\delta_{m0}) \left[\left(T^{0,\alpha}_{nm}\mathscr{D}^0_{n,\,m+1} + T^{1,\alpha}_{nm}\mathscr{D}^1_{n,\,m+1}\right) - \frac{n-m-1}{n(2n-1)}\left(P^{1,\alpha}_{nm}\mathscr{D}^0_{n-1,\,m+1} - P^{0,\alpha}_{nm}\mathscr{D}^1_{n-1,\,m+1}\right) \right\} - \frac{n+m}{4}(1-\delta_{m0}) \left[\left(T^{0,\alpha}_{nm}\mathscr{D}^0_{n,\,m-1} + T^{1,\alpha}_{nm}\mathscr{D}^1_{n,\,m-1}\right) \right. \right. \tag{A8}$$

$$+\frac{n+m-1}{n(2n-1)}\left(P^{1,\alpha}_{nm}\mathscr{D}^{0}_{n-1,m-1}-P^{0,\alpha}_{nm}\mathscr{D}^{1}_{n-1,m-1}\right)\Bigg]\Bigg\}$$

$$\mathscr{D}^{\beta}_{3}=\sum_{n=1}^{\infty}\sum_{m=0}^{n}\frac{1}{\lambda_{nm}}\Bigg\{(n-m)(1+\delta_{m0})\Bigg[\left(T^{0,\alpha}_{nm}\mathscr{D}^{0}_{n,m+1}+T^{1,\alpha}_{nm}\mathscr{D}^{1}_{n,m+1}\right)$$

$$-\frac{n-m-1}{n(2n-1)}\left(P^{1,\alpha}_{nm}\mathscr{D}^{0}_{n-1,m+1}-P^{0,\alpha}_{nm}\mathscr{D}^{1}_{n-1,m+1}\right)\Bigg\} \tag{A9}$$

$$-\frac{n+m}{4}(1-\delta_{m0})\Bigg[\left(T^{0,\alpha}_{nm}\mathscr{D}^{0}_{n,m-1}+T^{1,\alpha}_{nm}\mathscr{D}^{1}_{n,m-1}\right)$$

$$+\frac{n+m-1}{n(2n-1)}\left(P^{1,\alpha}_{nm}\mathscr{D}^{0}_{n-1,m-1}-P^{0,\alpha}_{nm}\mathscr{D}^{1}_{n-1,m-1}\right)\Bigg]\Bigg\}$$